IEEE Access
Multidisciplinary ⋮ Rapid Review ⋮ Open Access Journal

Received December 25, 2020, accepted January 7, 2021, date of publication January 11, 2021, date of current version January 21, 2021.

Digital Object Identifier 10.1109/ACCESS.2021.3050780

Energy Efficient and Safe Control Strategy for Electric Vehicles Including Driver Preference

SEPEHR G. DEHKORDI[1,2], MICHAEL E. CHOLETTE[3], GRÉGOIRE S. LARUE[1,2], ANDRY RAKOTONIRAINY[1,2], AND SÉBASTIEN GLASER[1,2]

[1]Centre for Accident Research Road Safety-Queensland (CARRS-Q), Queensland University of Technology (QUT), Brisbane, QLD 4059, Australia
[2]Institute of Health and Biomedical Innovation (IHBI), Queensland University of Technology (QUT), Kelvin Grove, QLD 4059, Australia
[3]Science and Engineering Faculty, Queensland University of Technology (QUT), Brisbane, QLD 4059, Australia

Corresponding author: Sepehr G. Dehkordi (sepehr.ghasemi@qut.edu.au)

This work was supported in part by the Australian Research Council Discovery under Grant DP140102895, and in part by the Queensland University of Technology (QUT).

ABSTRACT In this manuscript, a control strategy for electric vehicles is developed to optimise the energy consumption while respecting constraints associated with both inter-vehicle safety and comfort, which is a challenge in typical optimal control solution methodologies. Firstly, the long-term optimal control is developed using Pontryagin's Maximum Principle (PMP). Thereafter, the obtained PMP solution is used to bound the state space for a computationally tractable Dynamic Programming (DP) optimisation to ensure the satisfaction of the safety constraints. While the acceleration subproblem solution is similar to internal combustion engine vehicles (ICEVs), the combination of regenerative and hydraulic braking significantly alters the nature of the optimal braking profile. Since a DP solution is not tractable for real-time implementation of combined braking, a fast heuristic is developed, which achieves 98% of the optimal energy recovery calculated by the DP in the simulated cases. Simulation results demonstrate that the proposed strategy respects the acceleration and safety constraints while saving approximately 5% energy use without significantly increasing travel time. Further simulations were conducted to evaluate the effect of driver preferences on energy use. It was shown that a 9.5% reduction in energy use if the driver is willing to accept a 10% speed reduction.

INDEX TERMS Electric vehicle, model predictive control, Pontryagin maximum principle, dynamic programming.

I. INTRODUCTION

The transportation sector is responsible for 30% of global emissions across the world [1]. Electric Vehicles (EVs) have the potential to reduce the negative environmental impacts of the transport sector (particularly if these vehicles are charged using renewable energy). The market penetration of EVs has increased 57% in the past decade and it is expected grow rapidly until 2040 [2]. Yet, the main challenge with the uptake of EVs is their reduced range compared to internal combustion engine vehicles (ICEVs). While the range of EVs may be extended through new technologies (e.g. vibration energy harvesting) [3], driving style is also highly influential and can be improved by ecological driving (eco-driving).

Eco-driving consists of guidelines and driving methods based on rules of thumb, such as smooth deceleration, acceleration, and maintaining momentum to improve energy efficiency [4], [5]. The main disadvantage with these guidelines is that they provide general advice and cannot rigorously address the different EV dynamics and consider traffic condition to achieve the optimal performance. This issue can be overcome by defining eco-driving as an optimal control problem (OCP) where the vehicle dynamics and traffic conditions are considered to minimise energy consumption [6]–[9].

Model predictive control (MPC) is the most common approach to obtain energy efficient driving in dynamic traffic conditions [10]–[13]. MPC solves an optimisation of energy consumption within a short time horizon (e.g. 5 to 15 seconds) [12], [14]. In order to ensure the feasibility and safety of optimised trajectories, the optimal control subproblems in the MPC approach should consider constraints, including: i) physical constraints (e.g. range of torque, maximum braking force, maximum regenerative energy) and ii) safety constraints (e.g. feasible acceleration, speed limits,

The associate editor coordinating the review of this manuscript and approving it for publication was Shanying Zhu.

fixed distance [12], relative distance [15], and time to collision [16] with the preceding vehicle). Several optimisation techniques can be used to incorporate constraints when computing the optimum velocity profile such as nonlinear programming [15], dynamic programming [16], and Quadratic programming [17]. An important challenge in MPC is the consideration of constraints while ensuring a reasonable computation time/load for online deployment. Indeed, constraints are often ignored or weakened to achieve real-time solution which can produce unrealistic or unsafe results.

The second challenge to implementing MPC algorithms is to design a methodology that does not contain hard-to-tune parameters. Most of the optimisation frameworks have weighting factors to manage the trade-off between optimisation objectives such as travel time, energy consumption, and inter-vehicle safety [6], [18]–[20]. Setting the values of these weights is typically done by trial and error, and the weights often lack an easily interpretable meaning for the driver. Such an approach makes it difficult to guarantee safety in all conditions, as all scenarios may not have been considered to tune the weights. Therefore, it is concluded that there is a need for a transparent definition of the weights so that the algorithm can adapt to driver preference and current traffic conditions, without potentially adversely affecting safety.

The third challenge in designing MPC is selecting the horizon length, which should be as long as possible to obtain near-optimal solutions [12], [14]. However, increasing the length of the horizon increases the computational cost of the MPC optimisation solver, which has an impact on the real-time applicability of the MPC approach [21]. To increase the prediction horizon and keep the computational cost low, Han, *et al.* [12] proposed an MPC framework by solving PMP where safety is introduced as a fixed gap. However, their approach did not consider control bounds in the solution procedure and ignored the hydraulic brake input. While accurate long-term predictions could alleviate the need for extreme control sequences, changing traffic conditions make almost impossible to obtain an accurate prediction, necessitating the consideration of control constraints and hydraulic brakes to provide feasible solutions.

One approach used to reduce the necessity of accurate long-term traffic predictions is the use of a two-stage technique based on long-term optimisation and short-term adaptation. This method has been used for ICEVs, plug-in, and hybrid EV [17], [22], [20]. The long-term optimisation refers to optimising a long-horizon by assuming free-flow driving to adapt the speed to the upcoming traffic and topographical information of the road. The short-term adaptation refers to the use of MPC with safety constraints [20], [23]. Most of the existing research use numerical optimisers for long-term optimisation, which typically have high computation times. As a consequence, the reference trajectory can only be computed once at the start of the journey and updated occasionally, and thus the long-term velocity profile cannot adapt to dynamic traffic conditions, which degrades the performance of the MPC. Indeed, [16] and [24] show that if the reference trajectory cannot be updated in real-time, the number of hydraulic braking events and unnecessary accelerations is increased for the two-stage optimisation approach, and its performance is degraded significantly. To update the reference trajectory when traffic changes abruptly, an analytical solution with proper constraints is required (i.e. control constraints such as constraint on the torque and braking force).

Although there are studies addressing the analytical solution for EV longitudinal dynamics [7], [10], the vast majority of studies have ignored friction brakes [12], [25], [26]. In Jia, *et al.* [27], the authors include friction brake by applying numerous simplifications to the optimisation problem to provide a real-time solution, for instance by simplifying the maximum regenerative braking regions. Efficient and safe braking is achievable by considering maximum possible regenerative braking, reducing hydraulic brake, and real-time update of the long-term optimisation process.

This article aims to design a control strategy for EVs that minimises the energy consumption while respecting typical constraints associated with safety and comfort (TIV, TTC, acceleration range and speed limit). Similar to existing work, a two-stage optimisation approach is adopted from [6], [16] However, unlike previous work, this study uses an analytical solution for long-term optimisation to obtain real-time update and satisfaction of control (i.e. acceleration and hydraulic brake), with a short-term optimisation to consider inter-vehicle safety. The first stage provides a real-time control-constrained PMP solution for the long-term optimisation, and the second stage is a computationally tractable MPC framework with state-constraints to ensure the satisfaction of the inter-vehicle safety criteria. The contributions of this study are as follows:

- The use of an analytical solution for the optimisation of the long-term reference trajectory, which enables real-time updating of the reference trajectory rather than simply using the pre-trip reference.
- A methodology for near-optimum and real-time solution of the energy minimal control in the presence of safety and control constraints.
- Transparent inclusion of user preferences via a ''preference velocity'', which is the speed that the driver prefers when traffic and speed limits allow.

The remainder of the article is organized as follows. Section II provides an overview of the two-stage methodology, and Section III presents the EV model. Section IV describes the optimisation of the long-term reference trajectory via PMP, while Section V describes an MPC framework to adapt the long-term trajectory to respect safety constraints. Section VI presents a simulation case study and Section VII concludes the study and suggests possible avenues for future work.

II. METHODOLOGY

In this article, a two-stage optimisation framework is used for EVs to minimise energy usage. Fig.1 shows the overall methodology of the proposed approach, which includes: the

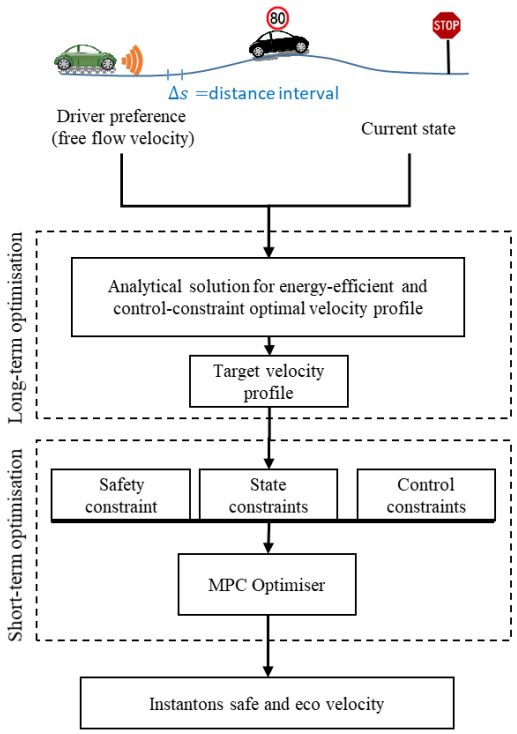

FIGURE 1. Methodology flowchart of proposed controlling EV.

long-term optimisation to obtain the most energy-efficient velocity profile, and the short-term optimisation, to consider inter-vehicle safety along with energy-efficient driving velocity.

The long-term optimisation uses the current state and the driver's preferred free-flow velocity to conduct the energy optimisation. The solution produces a target velocity profile which respects the control constraints and accelerates the vehicle to either the velocity of the preceding vehicle or the driver's preferred velocity. For the optimisation to be effective under dynamic traffic conditions, it is necessary to solve the long-term optimisation efficiently so that it can be updated in real-time.

Subsequently, the short-term optimisation is a look-ahead Eco and Safe (EcoSafe) MPC approach with control and state constraints related to EV dynamics. Here, the target velocity profile from the long-term optimisation is used to narrow the search space for finding instantaneous safe and eco velocity. The safety-related constraints, such as Time to Collison (i.e. relative distance divided by the relative speed) and Inter-vehicular time (TIV, relative distance divided by the ego vehicle speed), are considered as the constraints in the MPC formulation.

In the subsequent sections, the methodology is described in detail. In section IV, an analytical solution for EV dynamics is obtained by considering control constraints with the use of hydraulic, regenerative braking and the safe range for acceleration/deceleration. Then, this analytical solution is used in the design of a fast MPC optimiser section V.

III. ELECTRIC VEHICLE MODEL

In this section, the model for the EV is described in detail. While the dynamics of EVs can be quite complex, this study uses a simplified control-oriented model, as is typical in control studies of EVs and ICEs [12], [28], [29]. Consider the longitudinal motion for a vehicle [29], [30]:

$$\begin{aligned} F_w &= ma + c_0(\theta) + c_1(\theta)\, v + c_2 v^2 + F_b \\ c_0(\theta) &= 0.5 C_d \rho A v_w^2 + mg\left(c_{r,1}\cos(\theta) + \sin(\theta)\right) \\ c_1(\theta) &= c_{r,2} mg\cos(\theta) - C_d \rho A v_w^2 \\ c_2 &= 0.5 C_d \rho A + c_{r,3} mg\cos(\theta) \end{aligned} \tag{1}$$

where F_w[N] is the force on the wheel, a[m/s^2] is the acceleration, v[m/s] is the velocity, θ is the angle of the road slope angle, F_b [N] is the hydraulic brake and $c_{r,1}$, $c_{r,2}$ and $c_{r,3}$ are the rolling friction coefficients. C_d, ρ, A, v_w are the aerodynamic drag coefficient, the air mass density, the effective frontal vehicle area and the wind velocity, respectively. For notational simplicity, the term $c_0(\theta) + c_1(\theta)\, v + c_2 v^2$ can be expressed as a steady-state force (F_{ss}) applied on the wheel. Equation (1 can then be rewritten as:

$$F_w = ma + F_{ss}(v, \theta, v_w) + F_b \tag{2}$$

The relationship between the force on the wheel and the electric motor torque (T_m) is given by Han, *et al.* [12]:

$$F_w = \left(T_m \eta_t^{sign(T_m)} R_t\right)/r \tag{3}$$

where R_t is the transmission ratio, η_t is the transmission efficiency and r is the wheel radius. It should be noted that F_w has the same sign as T_m since η_t, R_t and r are positive values. The term $sign(T_m)$ is used to incorporate the efficiency of driveline for positive, negative and zero torques applied to the wheel. The power consumption can be obtained from the relationship between the voltage and current of the electric motor, which is equal to [7]:

$$P_e = V_a i_a = b_1 v T_m + b_2 T_m^2 \tag{4}$$

i.e. the relationship between P_e and T_m is quadratic. However, the torque is limited to be within the range $T_{m,min} \le T_m \le T_{m,max}$. The range of the motor torque is a common approach for considering the operational range of electric motors in EVs [7], [10].

Instead of using the motor torque as the control variable, the acceleration is considered as the control variable in this study. This choice is not too restrictive, since Eqs. (2) and (3) can be used to solve for the motor torque from the desired acceleration. Indeed, having acceleration as the control variable allows the specification of control constraints to limit unsafe and uncomfortable accelerations directly. In this study, the interval $[-4, 4]$ m/s^2 is considered as the allowable range of acceleration, which is similar to other studies [26], [31]. Fig. 2 shows the relationship between T_m, v and a (within the allowable acceleration range) when F_b is zero.

If $a > 0$, the maximum acceleration is bounded by the maximum torque (blue line in Fig. 2), which shows that

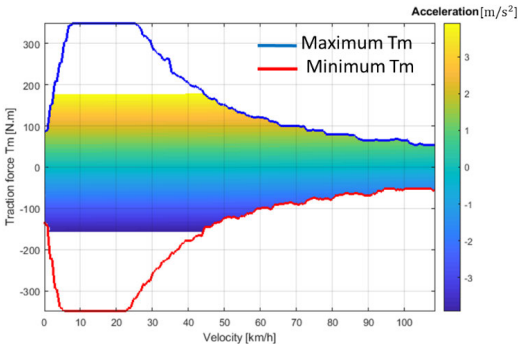

FIGURE 2. Relationship between traction force, velocity and acceptable range of acceleration for EVs specified in Table 1.

increasing the velocity reduces the maximum acceleration. If $a < 0$, the negative T_m can provide resistive force for reducing velocity. In this mode, the motor is used as a generator and can use some of the kinetic energy from the vehicle to charge the battery.

Fig. 2 shows the minimum acceleration necessary for regenerative braking ($a_{min,r}$) when the hydraulic braking F_b is zero. It is obviously preferable to use only regenerative braking to save energy since hydraulic braking transfers the kinetic energy to heat. However, to maintain safe operation, the combination of regenerative and hydraulic braking may be necessary. The optimum combination of regenerative braking and hydraulic braking, which results in the highest energy savings is the subject of section IV.B. The notation and parameter values used in this study are summarised in TABLE 1. In the next section, the long-term optimisation is developed for EVs. The problem is constrained within a safe acceleration range and propose a braking strategy to increase safety and maximise regenerative braking energy that combines hydraulic and regenerative braking.

IV. CONTROL CONSTRAINED OPTIMAL CONTROL PROBLEM FOR LONG-TERM OPTIMISATION

The long-term optimisation is used to identify the optimal speed profile with regard to the traffic conditions. As shown in Fig. 1, the purpose of the long-term optimisation is to determine the optimal control profile to reach the steady-state speed of the traffic ahead. For this study, the steady-state velocity is taken to be either the minimum of the average velocity of the preceding vehicle over a suitable time window (10s) or the driver preference velocity [24]. The optimal control statement of the long-term optimisation is given by:

$$\begin{aligned}\min_{a(t)} \int_0^{t_f} & [P_e(t) + \psi \\ & + \lambda_{c,max}\left(a - a_{max}(v)\right)^2 h\left(a - a_{max}(v)\right) \\ & + \lambda_{c,min}\left(a - a_{min}(v)\right)^2 h\left(a_{min}(v) - a\right)]dt\end{aligned}$$

Subject to $\dot{s} = v$

$$\dot{v} = a = \left(\frac{P_e}{v} - F_{ss} - F_b\right)/m$$

$$P_e = b_1 v T_m + b_2 T_m^2$$

TABLE 1. System Parameters [12]

Symbol	Quantity	Value
$c_{r,1}$	1st rolling friction coefficient	1.5
$c_{r,2}$	2nd rolling friction coefficient	0.1181
$c_{r,3}$	3rd rolling friction coefficient	4.575
c_d	Aerodynamic coefficient	1.05
ρ	Aerodynamic constant	1.2
A	Frontal mirror area	0.58 m^2
v_w	Wind velocity	1.0 m/s
R_t	transmission ratio	9.59
r	wheel radius	0.2820 m
η_t	Driveline efficiency	0.90
b_1	1st electric motor coefficient	34.007 m^{-1}
b_2	2nd electric motor coefficient	0.8730

$$\begin{aligned}& T_{m,min} \le T \le T_{m,max} \\ & 0 \le F_b \le \mathrm{F_{b,max}} \\ & v_0 \text{ and } v\left(t_f\right) \text{ known}\end{aligned} \tag{5}$$

where t_f is free, v_0 and $v\left(t_f\right)$ are initial velocity and final velocity, respectively. Since the target speed $v\left(t_f\right)$ is known, fixed final time formulations tend to over-constrain the solution by requiring a specific average acceleration to achieve the target $v\left(t_f\right)$. Instead, an indirect time penalty (ψ) is considered here to penalise excessively large final times. Methods to set ψ based on driver preferences are discussed later in this section.

The running cost is augmented with two penalty terms to (heavily) penalise violations of the control constraints. The two terms with the (large) weights $\lambda_{c,max}$ and $\lambda_{c,min}$ and the Heaviside function $h(\cdot)$ serve to penalise accelerations that are less than the lower acceleration bound a_{min} or greater than the maximum acceleration a_{max}. The Hamiltonian of this system is as follows:

$$\begin{aligned}\mathcal{H} := & P_e + \psi + (\lambda_s + \epsilon)v + \lambda_v a \\ & + \lambda_{c,max}\left(a - a_{max}(v)\right)^2 h\left(a - a_{max}(v)\right) \\ & + \lambda_{c,min}\left(a - a_{min,r}(v)\right)^2 h\left(a_{min,r}(v) - a\right)\end{aligned} \tag{6}$$

where λ_s and λ_v are the distance and velocity co-states and ϵ is an indirect distance penalty (which will be used later for braking with distances) [32]. The co-state differential equations for λ_v and λ_s are given by the well-known necessary optimality conditions [33]:

$$\begin{aligned}\dot{\lambda_v} &= -\frac{\partial \mathcal{H}}{\partial v} \\ \dot{\lambda_s} &= -\frac{\partial \mathcal{H}}{\partial s} = -\frac{\partial \mathcal{H}}{\partial \theta} \cdot \frac{\partial \theta}{\partial s}\end{aligned} \tag{7}$$

Equation (7) forms a nonlinear two-point boundary value problem (TPBVP) whose solution usually requires numerical techniques (e.g., multiple shooting methods) [12], [34]. The long-term optimisation is customarily split into acceleration

and deceleration modes with a free final time. An indirect method to solve the Pontryagin's Maximum Principle (PMP) described in previous studies will be used to solve for the optimal control [32], [35].

The optimal control must minimise the Hamiltonian function. If the Hamiltonian is continuous and differentiable in the control, then solving $\frac{\partial \mathcal{H}}{\partial a} = 0$ with respect to a yields the optimum acceleration [29], [32], [33]. Indeed, it can be seen that the Hamiltonian in Equation (6) is a continuous function since $\mathcal{H}\left(a_{min}^{-}\right) = \mathcal{H}\left(a_{min}^{+}\right)$ and $\mathcal{H}\left(a_{max}^{-}\right) = \mathcal{H}\left(a_{max}^{+}\right)$. The derivative of the Hamiltonian with respect to a is:

$$\begin{aligned} \frac{\partial \mathcal{H}}{\partial a} &= 0 \\ &= \frac{dP_e}{da} + \lambda_v \end{aligned} \tag{8}$$

where $\frac{dP_e}{da}$ is equal to

$$\begin{aligned} \frac{dP_e}{da} = &\frac{2\mathrm{b}_2 mr^2 \left(F_{ss} + F_b + am\right)}{R_t^2 \eta_t^{2\mathrm{k}}} + \frac{b_1 mrv}{R_t \eta_t^k} \\ &+ 2\lambda_{c,max} \left(a - a_{max}\left(v\right)\right) h\left(a - a_{max}\left(v\right)\right) \\ &+ 2\lambda_{c,min} \left(a - a_{min}\left(v\right)\right) h\left(a_{min}\left(v\right) - a\right) \\ &+ \lambda_{c,max} \left(a - a_{max}\left(v\right)\right)^2 \delta\left(a - a_{max}\left(v\right)\right) \\ &+ \lambda_{c,min} \left(a - a_{min}\left(v\right)\right)^2 \delta\left(a_{min}\left(v\right) - a\right) \end{aligned} \tag{9}$$

The term $\delta(\cdot)$ is the Dirac Delta function (which is the derivative of $h(\cdot)$) and $k \triangleq sign\left(T_m\right)$. Noting that $x\delta(x) = 0 \forall x$, the last two terms can be eliminated and Equation (9) can be substituted into Equation (8) to obtain the following expressions for the extremal control a:

If $a_{min} \le a \le a_{max}$:

$$a = -\frac{\lambda_v}{m\frac{2\mathrm{b}_2 mr^2}{R_t^2 \eta_t^{2k}}} - \frac{\frac{b_1 mrv}{R_t \eta_t^k}}{m\frac{2\mathrm{b}_2 mr^2}{R_t^2 \eta_t^{2k}}} - \frac{\left(F_{ss} + F_b\right)}{m} \tag{10a}$$

If $a \le a_{min}$:

$$a = f_{a_{min}}\left(\lambda_v\right) = \mathrm{A}_0 \lambda_v + \mathrm{A}_1 + \mathrm{A}_2 a_{min}\left(v\right) \tag{10b}$$

If $a \ge a_{max}$:

$$a = f_{a_{max}}\left(\lambda_v\right) = \mathrm{B}_0 \lambda_v + \mathrm{B}_1 + B_2 a_{max}\left(v\right) \tag{10c}$$

$$\begin{aligned} A_0 &= -\frac{R_t^2 \eta_t^{2k}}{\left(2\mathrm{b}_2 m^2 r^2 + 2\lambda_{c,min} R_t^2 \eta_t^2\right)} \\ A_1 &= -\frac{R_t \eta_t b_1 mrv + 2\mathrm{b}_2 mr^2 \left(F_{ss} + F_b\right)}{\left(2\mathrm{b}_2 m^2 r^2 + 2\lambda_{c,min} R_t^2 \eta_t^{2k}\right)} \\ A_2 &= \frac{2R_t^2 \eta_t^{2k}}{\left(\frac{2\mathrm{b}_2 m^2 r^2}{\lambda_{c,min}} + 2R_t^2 \eta_t^{2k}\right)} \end{aligned} \tag{10d}$$

$$\begin{aligned} B_0 &= -\frac{R_t^2 \eta_t^{2\mathrm{k}}}{\left(2\mathrm{b}_2 m^2 r^2 + 2\lambda_{c,max} R_t^2 \eta_t^{2\mathrm{k}}\right)} \\ B_1 &= -\frac{R_t \eta_t^k b_1 mrv + 2\mathrm{b}_2 mr^2 \left(F_{ss} + F_b\right)}{\left(2\mathrm{b}_2 m^2 r^2 + 2\lambda_{c,max} R_t^2 \eta_t^{2\mathrm{k}}\right)} \\ B_2 &= \frac{2R_t^2 \eta_t^{2\mathrm{k}}}{\left(\frac{2\mathrm{b}_2 m^2 r^2}{\lambda_{c,max}} + 2R_t^2 \eta_t^{2\mathrm{k}}\right)} \end{aligned} \tag{10e}$$

If $\lambda_{c,max}$, $\lambda_{c,min}$ are large enough (ideally $\lambda_{c,max} = \lambda_{c,min} \to \infty$), then Equation (10) can be approximated by:

$$a \approx \begin{cases} a_{min}\left(v\right) & a_{min} \ge a \\ \mathrm{C}_1 \lambda_v + \mathrm{C}_2 - \dfrac{\left(F_{ss} + F_b\right)}{m} & a_{min} < a < a_{max} \\ a_{max}\left(v\right) & a \ge a_{max} \end{cases}$$

$$\mathrm{C}_1 = -\frac{R_t^2 \eta_t^{2\mathrm{k}}}{2\mathrm{b}_2 r^2}, \quad \mathrm{C}_2 = -\frac{\left(R_t \eta_t^{\mathrm{k}}\right)\left(b_1 rv\right)}{\left(2\mathrm{b}_2 mr^2\right)} \tag{11}$$

Since the problem is considered as a free-final time, the value of Hamiltonian must be equal to zero at an extremal trajectory [33]. Substituting λ_v in Equation (6) and considering $\mathcal{H} = 0$ gives the following necessary condition:

$$\begin{aligned} &P_e\left(a, v\right) + \psi + \left(\lambda_s + \epsilon\right)v + \lambda_v a \\ &\quad + \lambda_{c,max} \left(a - a_{max}(v)\right)^2 h\left(a - a_{max}(v)\right) \\ &\quad + \lambda_{c,min} \left(a - a_{min}\left(v\right)\right)^2 h\left(a_{min}\left(v\right) - a\right) = 0 \end{aligned} \tag{12}$$

Solving Equation (12) with respect to λ_v yields the relation between the optimum λ_v and a.

$$\lambda_v = -\frac{\begin{array}{c} P_e\left(a, v\right) + \psi + \left(\lambda_s + \epsilon\right)v \\ +\lambda_{c,max} \left(a - a_{max}\left(v\right)\right)^2 h\left(a - a_{max}\left(v\right)\right) \\ +\lambda_{c,min} \left(a - a_{min}\left(v\right)\right)^2 h\left(a_{min}\left(v\right) - a\right) \end{array}}{a} \tag{13}$$

Substituting λ_v from Equation (13) into Equation (11), and re-arranging the right side of Equation (11) with respect to a, yields the optimal acceleration with respect to λ_s:

$$a^* = \begin{cases} a_{min}\left(v\right) & a_{min} \ge a \\ \pm\sqrt{\dfrac{\begin{array}{c} D_0 F_{ss}^2 + \mathrm{D}_1 v\left(F_{ss} + F_b\right) \\ +\mathrm{D}_2 \psi + \mathrm{D}_2 v\left(\lambda_s + \epsilon\right) \end{array}}{\mathrm{D}_3}} & a_{min} < a < a_{max} \\ a_{max}\left(v\right) & a \ge a_{max} \end{cases} \tag{14a}$$

$$\begin{aligned} &D_0 = b_2 r^2, \quad \mathrm{D}_1 = R_t b_1 \eta_t^k r, \ \mathrm{D}_2 = R_t^2 \eta_t^{2k} \\ &D_3 = b^2 m^2 r^2 \end{aligned} \tag{14b}$$

The value of co-estate λ_s is obtained by assuming a relaxed condition for the final time $a^*\left(t_f\right) = 0$ with v equal to the steady-state velocity v_{ss} (i.e. $v(t_f) = v_{ss}$) and a constant slope angle for the upcoming horizon[1]:

$$\begin{aligned} \mathcal{H}\left(t_f\right) = 0 = D_0 P_{ss}^2\left(v_{ss}\right) + \left(\mathrm{D}_1 v_{ss}\right) P_{ss}\left(v_{ss}\right) + \mathrm{D}_2 \psi \\ + D_2 v_{ss}\left(\lambda_s + \epsilon\right) \end{aligned} \tag{15}$$

λ_s can be obtained by solving Equation (15):

$$\lambda_s = -\frac{b_1 \frac{\left(rv_{ss}\right) F_{ss}\left(v_{ss}\right)}{R_t \eta_t^k} + b_2 \frac{r^2 F_{ss}^2\left(v_{ss}\right)}{R_t^2 \eta_t^{2k}} + \psi}{v_{ss}} - \epsilon \tag{16}$$

The magnitude of the right side of Equation (16) is related to the energy consumption per distance at v_{ss}, modified by the

[1]This condition enables cruising after the acceleration maneuver is terminated.

time penalty ψ. Since the optimum policy should minimise the Hamiltonian and co-states, the value of ψ should also minimise Equation (16). Since $\frac{P_e}{v}$ is convex in v, the value of ψ that minimises Equation (16) is as follows [32]:

$$\left.\frac{\partial \frac{P_e(a=0,v)+\psi}{v}}{\partial v}\right|_{v=v_{ss}} = 0 \tag{17}$$

Solving Equation (17) gives the indirect time penalty ψ for a specific preference velocity. Indeed, instead of considering t_f to obtain the velocity profile, which is difficult to localise based on traffic conditions and hard to interpret for the driver, the upcoming traffic velocity or comfort velocity v_c is used to obtain a reference trajectory. If the driver intention is to drive at any desired velocity, the ψ value can be obtained from Eq. (17) when $v_{ss} = v_c$. Solving Eq. (17) for $\psi = 0$ returns the optimum steady-state velocity (v_{opt}). Cruising at v_{opt} provides a lower energy consumption and longer range. For the EV dynamics reported in Table 1, v_{opt} is equal to 18 km/h.

Equation (14) shows that the driving scenario can be divided into $a \geq 0$ and $a < 0$ by considering the $\pm$ sign before the square root operator. In addition, the hydraulic brake, F_b in Equation (14) needs to be determined. The subject of the next two sections is to describe how the velocity profile and the control parameters are obtained from Equation (14) under different acceleration and deceleration scenarios.

A. ACCELERATION MODE ($a \geq 0$)

In the acceleration mode ($v_0 \leq v_{ss}$), the minimum acceleration is a_{min} in Equation (14) equals to zero, and $k = 1$. Since in this mode $F_b = 0$, the optimal policy of control to reach v_{ss} is given by:

$$a^* = \begin{cases} 0 & a \leq 0 \\ \sqrt{\dfrac{D_0F_{ss}^2 + D_1v\,(F_{ss}) \\ +D_2\psi + D_2v\,(\lambda_s + \epsilon)}{D_3}} & 0 < a < a_{max} \\ a_{max}\,(v) & a \geq a_{max}(v) \end{cases} \tag{18}$$

Equation (18) is a simple representation of an acceleration problem with control constraints. The distance penalty ϵ is included for the sake of generality and can be used for cases where the acceleration distance is limited (e.g., merging). In this article, $\epsilon = 0$ for the acceleration case without loss of generality. In the case of limited-distance acceleration, this penalty can be determined using a simple line search. This simplicity represents a key advantage of the proposed method compared to state of the art: the line search replaces multiple shooting methods [7], [12] to solve a two-point boundary value problem.

B. DECELERATION MODE ($a \leq 0$)

The deceleration problem is complicated beyond what is typically considered in eco-driving, given that it involves the introduction of regenerative braking. Since λ_s and ψ are constant values in the Hamiltonian, increasing ψ can increase the average speed and, consequently, increase energy consumption. Therefore only λ_v has an influence when minimising the Hamiltonian.

Unlike the acceleration case, deceleration nearly always comes with a finite distance (e.g. slowing down for a new speed limit, coming to a stop at an intersection). The final distance is handled using an indirect distance penalty ϵ which needs to be calculated for a specific distance and can be obtained using a line search [32].

To find λ_v, $a(t)$ must be identified forthe three different modes:

i. If $T_m > 0$ and $a \leq 0$, deceleration is occurring while consuming energy from the battery. In this case, $0 < T_m \leq \frac{\eta_t rmF_{ss}}{mR_t}$. This mode is not considered since it is clearly suboptimal (we know energy can be saved with regeneration braking).
ii. If $T_m = 0$, coasting is occurring and $a^* = -F_{ss}/m$.
iii. If $T_m < 0$, regenerative braking is occurring. In this mode, the electric motor is driven to charge the battery from the deceleration of the vehicle.

The optimum deceleration is a combination of possible deceleration modes including regenerative braking, coasting and hydraulic braking. [7] shows that three modes of braking can be encountered: 'Regenerative braking + hydraulic braking' (RHB), 'Only regenerative braking' (RB) and 'Coasting + regenerative braking' (CRB). In the following subsection, we develop a heuristic Pontryagin's Maximum Principle (PMP)-based approach for these three deceleration modes for long-term optimisation with control constraints.

1) DECELERATION WITH ONLY REGENERATIVE BRAKING

This mode is similar to $a^* \geq 0$ when the control is acceleration and $F_b = 0$ and $a_{min} = a_{min,r}$. In this mode, T_m has a negative value and $sign\,(T_m) = -1$. Since increasing the time penalty ψ results in increasing both the average velocity and energy consumption, ψ is set to zero in the deceleration mode. In addition, $a_{max} = 0$ and the term $h\,(a - a_{max}\,(v))$ is not an active constraint and it is given by Equation (19).

$$a^* = \begin{cases} a_{min,r}\,(v) & a \leq a_{min,r}(v) \\ -\sqrt{\dfrac{D_0F_{ss}^2 + D_1vF_{ss} \\ +D_2\psi + D_2v\,(\lambda_s + \epsilon)}{D_3}} & a_{min} < a < 0 \\ 0 & a \geq 0 \end{cases} \tag{19}$$

The deceleration scenario is defined for a specific distance to reach v_{ss}. The distance penalty ϵ is obtained using an exact line search (e.g., Fibonacci search) to achieve a specified final distance s_e, which is found from either 1) the desired final gap with the preceding vehicle or 2) the distance required for decelerating from a higher to a lower speed limit. If $\epsilon = 0$, the vehicle first decelerates to v_{opt} and then coasts on that

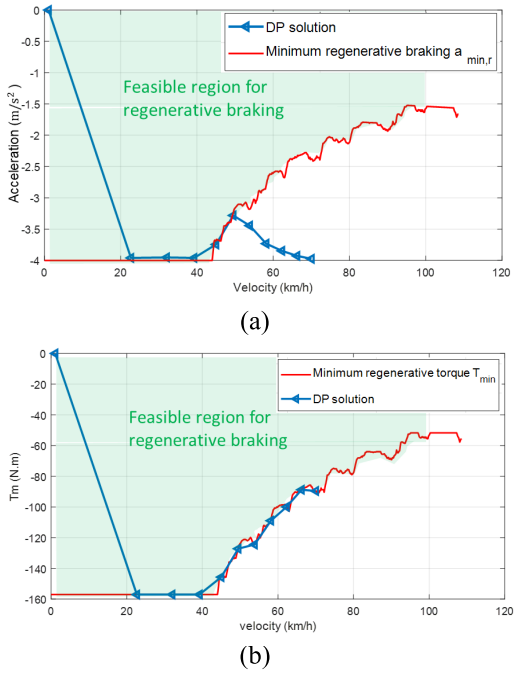

FIGURE 3. Deceleration scenario for 70 km/h to 0 in 60 m using DP.

velocity. This is because the solution is calculated with a free final time condition and the best energy consumption per distance is attainable when a vehicle is driving at its optimum speed.

2) DECELERATION CONSIDERING HYDRAULIC BRAKING

Hydraulic braking is not an ideal choice for optimum energy deceleration since it transfers the kinetic energy into heat. However, when regenerative braking is insufficient to avoid a safety constraint violation, hydraulic braking must be used to reduce velocity. Since the use of hydraulic brakes is more likely in safety critical scenarios, fast calculation is of paramount importance. To consider hydraulic braking F_b and ensure fast calculation, a one-dimensional auxiliary optimisation problem is solved which seeks to approximate the optimal solution while satisfying the final distance constraint. In the following, this procedure is discussed and the solutions is compared to the true (but not implementable) optimal solution, which is found via dynamic programming.

To motivate further developments, consider the following scenario where hydraulic braking is required: the deceleration from 70km/h to zero for vehicle dynamics is presented in Table 1. For this vehicle, hydraulic braking is required if $s_e < 60$m. Fig. 3 shows the optimum deceleration from 70 km/h to zero obtained via distance-based dynamic programming (DP) using the method from [16] with a 5 m step size. It can be seen that T_m is driven to the boundary to regenerate maximum energy. However, to attain this value, a^* is less than $a_{min,r}$, which necessitates hydraulic braking. When $v \approx 50\,km/h$, the deceleration may be achieved using only regenerative braking and the optimal

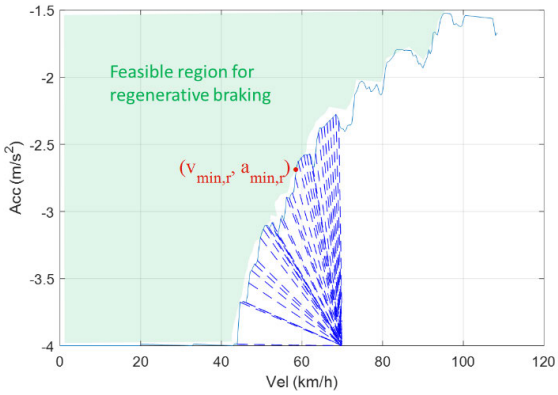

FIGURE 4. Linear search to reach the acceleration boundary for regenerative braking.

acceleration can be found using the regenerative only method from Section IV.B.1.

A method to mimic this behaviour will now be discussed which can provide a close-to-optimal solution while avoiding the computationally complex DP. Firstly, a heuristic is developed to manage the deceleration with hydraulic braking into the regenerative braking only feasible zone. Once this zone is achieved the remaining deceleration with only regenerative braking may be found via the PMP solution in Equation (19). The quality of the proposed method is evaluated using a simulation for a different scenario in section VI.

Motivated by the DP results in Fig. 3, it is assumed that the acceleration outside the feasible region follows a linear relationship with the vehicle velocity as illustrated in Fig. 4:

$$\bar{a}\,(v) = k_i\left(v - v_{\min,r}\right) + a_{min,r} \tag{20}$$

where $\left(v_{min,r}, a_{min,r}\right)$is a selected point on the regenerative-braking–only feasible region (i.e. the red curve in Fig. 3a). Once this point is selected, the slope can be computed as

$$k_i = \frac{a_0 - a_{min,r}}{v_0 - v_{min,r}}$$

Plugging Eq. (20) into the vehicle dynamics yields:

$$\dot{v} = \bar{a}\,(v) = k_i\left(v - v_{\min,r}\right) + a_{min,r} \tag{21}$$

which is a linear differential equation. Without loss of generality, consider the case where $t = 0$ is the beginning of the braking event. Eq. (21) may be solved with initial condition $v\,(0) = v_0$ to obtain:

$$v\,(t) = \alpha + \beta e^{-kt} \tag{22}$$

where $\alpha \triangleq \frac{a_{min,r}+kv_{min,r}}{k}$ and $\beta \triangleq \frac{kv_0 - a_{min,r} - kv_{min,r}}{k^2}$. Note that because of the definition of $\bar{a}(v)$ in Eq. (20), the velocity will achieve $v\,(t_1) = v_{min,r}$ at some future time t_1. After t_1, the PMP regenerative-braking-only solution becomes feasible and the method developed in Section B can be applied for $t \geq t_1$. To find the time where the PMP solution is active, let $v\,(t_1) = v_{min,r}$ in Eq. (22), which can be solved to obtain t_1:

$$t_1 = -\frac{1}{k} \cdot \ln\left[\frac{a_{min,r}}{a_{min,r} + kv_{min,r} - kv_0}\right] \tag{23}$$

Algorithm 1 Algorithm for Obtaining Close-to-Optimal Braking ($\hat{a}$)

Input: v_0, v_c, s_e
Output: $\hat{a}(t)$
Let $a^*_{PMP}(v_0, v_f, s)$ denote the control trajectory obtained via the PMP braking solution from Section IV.B with initial velocity v_0, final velocity v_f and final distance s.

If PMP solution is feasible with v_0, v_c, s_e:
$a(t) \leftarrow a^*_{PMP}(v_0, v_c, s_e)$
Else (hydraulic brakes needed)**:**
$Energy \leftarrow 0$
For $(v_{min,r}, a_{min,r})$ on the RB-only boundary:
$\bar{a}(t) = k_i\alpha + k_i\beta e^{-kt} - k_i v_{\min,r} + a_{min,r}$
$t_1 = -\frac{1}{k} \cdot \ln\left[\frac{a_{min,r}}{a_{min,r}+kv_{min,r}-kv_0}\right]$
$s(t_1) = \alpha t_1 + \beta\left(1 - e^{-kt_1}\right)$
$a(t) = \begin{cases} \bar{a}(t) & t < t_1 \\ a^*_{PMP}(v_{min,r}, v_c, s_e - s(t_1)) & t \geq t_1 \end{cases}$
Compute energy recovered $\rightarrow E$
If $E \geq Energy$
$Energy \leftarrow E$
$\hat{a}(t) \leftarrow a(t)$
End If
End For

End If

The distance where the PMP solution starts may then be obtained by integrating Eq. (22) and evaluating the resulting expression at time $t = t_1$:

$$s(t_1) = \alpha t_1 + \beta\left(1 - e^{-kt_1}\right) \tag{24}$$

The remainder of the control arc can be obtained via PMP with $v_0 \leftarrow v_{min,r}$ and $s_e \leftarrow s_e - s(t_1)$ (i.e. with the final distance decreased by the amount required to reach the regenerative-braking-only feasible region). Other hard braking scenarios are similar; they can be divided into regenerative-and-hydraulic-braking and regenerative-braking-only sub arcs. The regenerative-braking-only sub arc solution can be found with the PMP solution detailed in Section IV-B.1.

The remaining issue is the selection of the entry point to the regenerative-braking-only feasible region $(v_{min,r}, a_{min,r})$. This point is selected via a grid search along points on the feasible region boundary. The solution with the maximum energy recovery is selected. The overall algorithm for determining the close-to-optimal acceleration is summarised in Algorithm I.

When $\hat{a}$ is obtained with Algorithm 1, F^*_b is given by:

$$F^*_b = \begin{cases} \frac{\left(T_{min}\eta_t^{-1}R_t\right)}{r} - m\hat{a} - F_{ss} & a_{min} \leq \hat{a} < a_{min,r} \\ 0 & a_{min,r} \leq \hat{a} \leq 0 \end{cases} \tag{25}$$

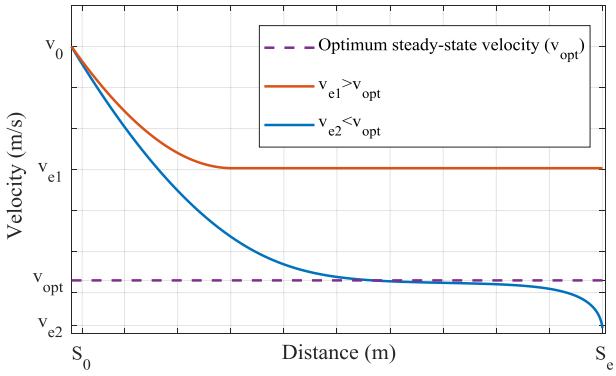

FIGURE 5. Optimum deceleration shape when the final terminal s_e is large when $v_{e1} < v_{opt}$ (Blue line) and $v_{e2} > v_{opt}$ (Red line).

The braking solution from Equation ((25) will later be compared with DP in section VI to evaluate how close the proposed method is to the optimum solution.

3) DECELERATION USING COASTING AND REGENERATIVE BRAKING

When deceleration can be performed over a long distance, the optimal regenerative braking solution may result in a low velocity for an excessive time. While this solution maximises energy recovery, such a solution may yield trajectories with extended cruising at low velocities and may not be acceptable in terms of safety and traffic considerations. Fig. 5 shows the two general cases of deceleration profile calculated by PMP i) when final velocity $v_{e1} > v_{opt}$ (red line), and ii) when final velocity $v_{e2} < v_{opt}$ (blue line).

The normal behaviour in deceleration is when $v_{e1} \geq v_{opt}$ where the vehicle decelerates to v_{e1} and maintains a constant velocity. However, when $v_{e2} < v_{opt}$ the vehicle decelerates to v_{opt}, cruises at this velocity, and subsequently conducts a second deceleration to reach the v_{e2}. Although both deceleration profiles recover maximum energy (i.e., it is optimal), the excessive cruising at the (low) optimal velocity is undesirable in many situations and may have safety and/or traffic consequences. Therefore, a coasting phase is proposed at the beginning of the solution to eliminate cruising at the lower velocity.

In the proposed method, the vehicle first coasts and then uses regenerative braking. Let t_2 be a specified coasting time at the beginning of the braking manoeuvre and denote the distance and velocity at the end of this coasting period as s_e and v_{e2}, respectively. The velocity and distance under coasting can be found by solving the differential equation

$$\ddot{s} = \dot{v} = -\frac{F_{ss}(v)}{m} \tag{26}$$

with the initial conditions $v(0) = v_0$ and $s(0) = 0$. The distance s_2 and velocity can be found by evaluating these solutions at t_2. After the coasting event, the PMP method is used to solve for the optimal deceleration from v_{e2} to v_e within the distance $s_e - s_2$.The coasting time t_2 is determined via a

grid search on the coasting time t_2 such that no cruising occurs (i.e. $|a(t)| < \varepsilon$ for some small ε).

V. SHORT-TERM OPTIMISATION USING MODEL PREDICTIVE CONTROL

In this section, the long-term optimisation trajectory derived in the previous section is used as the reference trajectory in an MPC framework. To localise the solution, the optimal control problem is formulated as a nonlinear spatial trajectory optimisation problem, seeking to minimise energy consumption over the distance horizon. Using the distance-based formulation, the cost for a distance step of Δs is given by:

$$\zeta = \frac{P_e + \psi}{v} \Delta s \tag{27}$$

which yields the MPC optimum control problem:

$$\begin{aligned} \min_{a_{k+1}, a_{k+2}, \ldots, a_{k+m-1}} & \sum_{i=0}^{i=p-1} \zeta_{k+i|k} \\ \text{subject to: } & v_{k+i+1|k} = v_{k+i|k} + a_{k+i|k}\,(\Delta t) \\ & T_{min} \le T_{k+i|k} \le T_{max} \\ & 0 \le v_{k+i|k} \le v_{tr,k+i|k} \\ & a_{min} \le a_{k+i|k} \le a_{max} \\ & G_{p,k+i|k} \ge v_{k+i|k} TIV_{min} + \ell \\ & G_{p,k+i|k} \ge \left(v_f - v_{pr}\right) TTC_{min}|_{v_f > v_{pr}} \end{aligned} \tag{28}$$

where $p\Delta s$ is the distance horizon, G_p is the gap with the preceding vehicle, ℓ is the minimum gap with the preceding vehicle,v_{pr} is the preceding vehicle's velocity, v_f is the following vehicle's velocity, TIV_{min} and TTC_{min} are the minimum inter-vehicle time and minimum time to collision, respectively.

v_{tr} in Equation (28) is the target velocity, and it is calculated using analytical solutions developed in section IV. v_{tr} is the upper limit of the velocity range and represents driving in free-flow conditions (i.e., TTC_{min} and TIV_{min} are not active constraints).

Maintaining an appropriate following distance with the preceding vehicle is the main safety issue, which is quantified by both the TIV and TTC, respectively. If the safety constraints are activated, the MPC obtains the speed profile satisfying the constraints associated with the traffic changes and EV dynamics. The TTC constraint is defined when the velocity of the following vehicle is greater than that of the preceding vehicle, which makes this constraint nonlinear. To ensure the satisfaction of safety constraints related to inter-vehicle safety, the modified distance base dynamic programming (MDDP) from [16] is employed. In addition to G_p, respecting speed limits and limiting the range of acceleration / deceleration are also constraints included in the proposed approach to ensure safety. For more details on the MDDP optimiser, the interested reader is referred to [16].

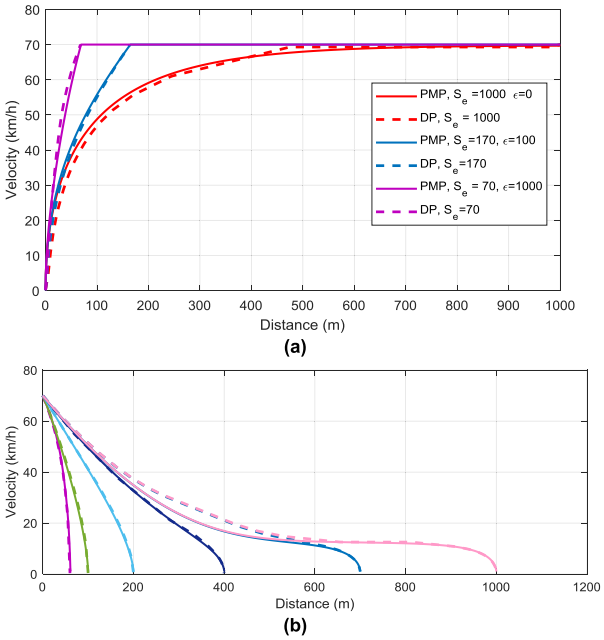

FIGURE 6. a) Comparison between proposed PMP and DP for acceleration scenario 0 to 70 km/h, b) Deceleration scenario from 70 km/h to 0 with different deceleration distances for proposed PMP solution (solid line) and DP (dashed line).

VI. SIMULATION RESULTS AND DISCUSSION

In this section, the PMP-based solution for long-term optimisation is first compared to the benchmark (DP) for different eco-driving sub-problems, including acceleration, deceleration using regenerative braking and deceleration using hydraulic braking. Then, the benefit of the EcoSafe-MPC is tested for a scenario with different speed limits and driver preference, to evaluate the effectiveness of the proposed method.

A. ACCELERATION FOR LONG-TERM OPTIMISATION

The acceleration profile based on the PMP formulation has two penalties: time ψ and distance ϵ. The ψ value was obtained from the desired steady-state velocity and Equation (17). The value of ϵ represents the distance penalty for scenarios in which the vehicle needs to reach a specific speed within a specific distance (e.g., merging) and is calculated during a braking manoeuvre. Fig. 6(a) shows the comparison between DP and the proposed PMP-based solution. It is observed that the results are very close to DP, and the difference can be attributed to the quantisation error introduced when using DP. The distance penalty increases energy consumption because of the increased acceleration to reach s_e.

B. DECELERATION SCENARIOS

The proposed PMP method is evaluated in a simple deceleration scenario. We compare the proposed PMP solution to the optimum solution calculated by DP to verify our findings. It is demonstrated that the defined constrains is always considered in the proposed method.

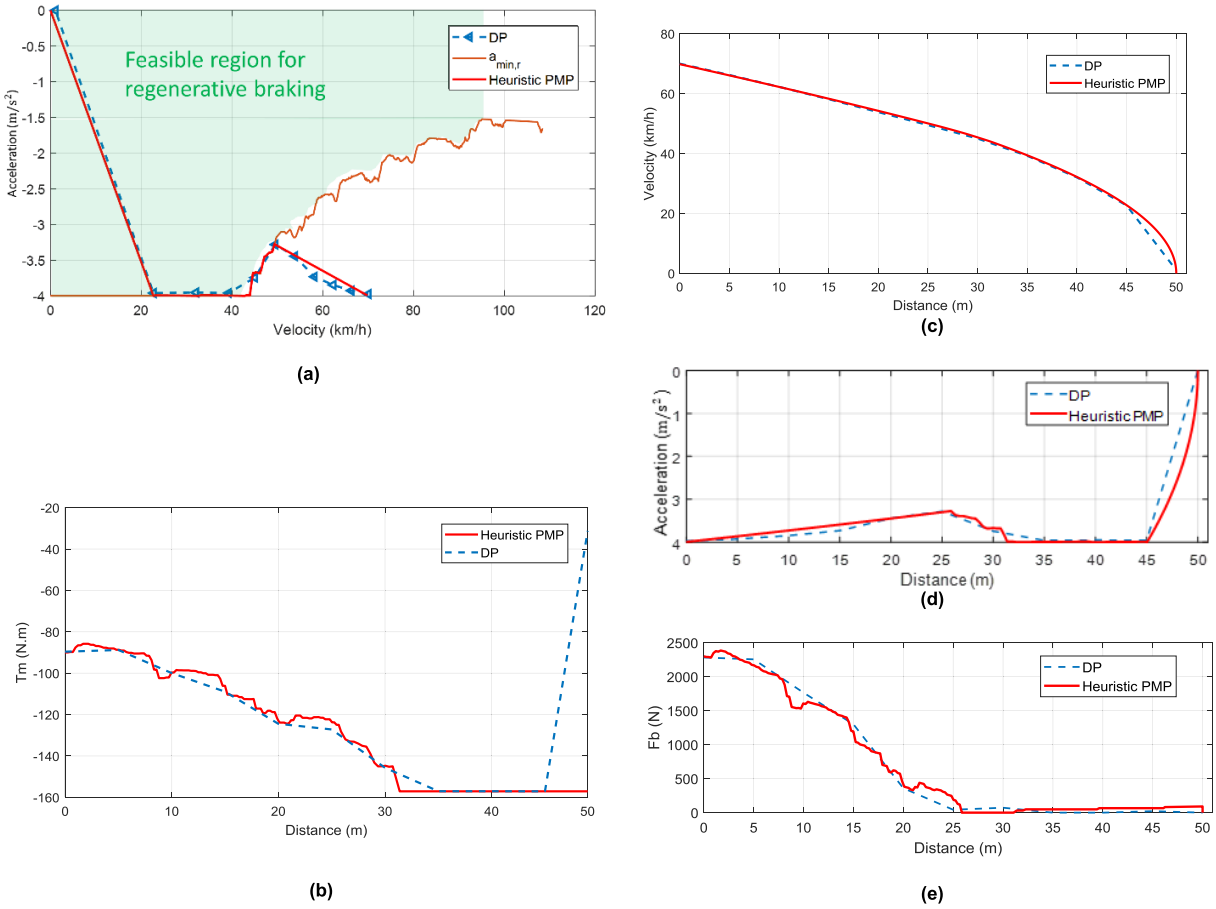

FIGURE 7. Comparison of proposed sub-optimal solution with DP for deceleration scenario (70 km/h to 0 in 60 m).

1) DECELERATION WITH ONLY REGENERATIVE BRAKING

Here, only regenerative braking is used to decelerate from v_0 to v_s. Fig. 6(b) shows the solutions using PMP and DP. Both approaches provide similar results, showing that the proposed sub-optimal solution is quite close to the optimal solution calculated via DP.

It is also observed that increasing the deceleration distance results in driving at a lower velocity (15 km/h), which increases the travel time. The minimum distance to decelerate without using regenerative braking is bounded by the minimum acceleration $a_{r,min}$. For example, Fig. 6(b) shows that deceleration from 70 km/h to zero within 60 m requires an acceleration less than $a_{r,min}$ and thus hydraulic brakes are necessary to reach the final condition. The proposed blended braking method described in section IV.B.2 is evaluated in the next section.

2) DECELERATION USING REGENERATIVE AND HYDRAULIC BRAKING

Fig. 7 shows the comparison of solutions using DP and the proposed method with deceleration scenario in Fig. 3. It is observed that the proposed method has comparable performance compared to the optimal solution, but has the advantage of fast calculation (0.03 seconds) with lower memory usage compared to DP, which has 23 seconds' computation time. The proposed deceleration solution is evaluated with different initial speeds in Fig. 8. The asterisks show the minimum distance that the vehicle can stop without using the hydraulic brakes. It is observed that, when only using regenerative braking, more distance is required to stop the vehicle. Furthermore, the distance where regenerative braking achieves the maximum energy recovery is close to the boundary where hydraulic braking would be required. This result implies that when braking at the maximum energy recovery point, a slight drop in the braking distance may require the use of the hydraulic brakes (and therefore waste energy). Also, the slope of the energy recovery curve is shallow to the right of the maximum, so there is little energy recovery penalty for braking over slightly longer-than-optimum distances. Thus, it may be desirable to plan to brake over longer distances to produce decelerations that recover near-maximum energy and are robust to small changes in the distance required to brake (e.g. due to misjudgement of the driver or changes in preceding vehicle motion).

Further analysis has been done to identify the optimality of the proposed heuristic in Algorithm I. Since DP suffers from

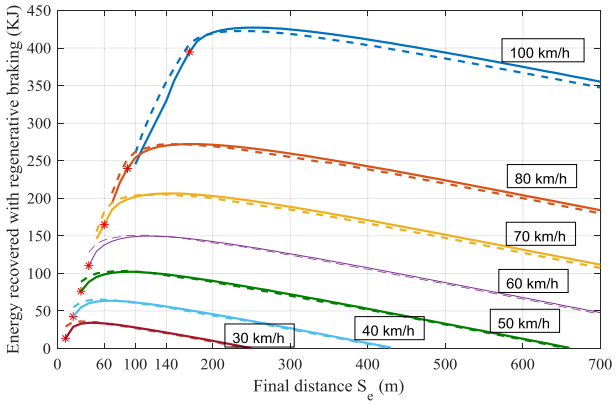

FIGURE 8. Energy produced by regenerative braking obtained from decelerating from 100, 80, 70, 60, 50, 40 and 30 km/h to 0 with different final distance. Solid line: proposed PMP. Dashed line: DP.

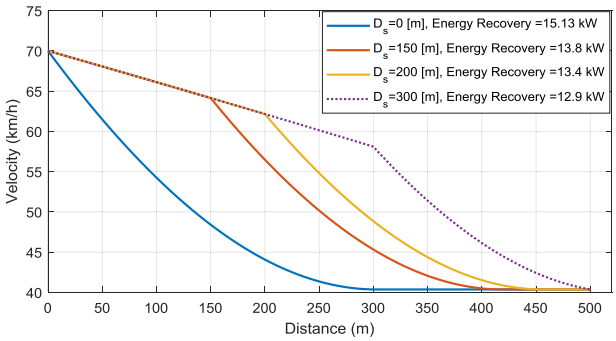

FIGURE 9. The impact of the proposed coasting strategy on speed profile and recovered energy: deceleration from 70 to 40 km/h.

discretisation errors, the proposed PMP recovers more energy compared to DP when only regenerative braking is used, i.e. $F_b = 0$. When the hydraulic brake is necessary (left side of "$*$" in each energy curve), the trends show a comparable result with DP and the produced energy is close to the DP solution. A Monte Carlo simulation was conducted by considering several initial velocities and deceleration distances. The results show that the proposed sub-optimal solution for regenerative braking recovers 98% of the optimal energy recovery (found using DP) when $F_b \neq 0$.

3) COASTING AND REGENERATING

To show the impact of the proposed coasting heuristic (Section IV-B3 on regenerative braking, a scenario is considered where the speed limit changes from 70 to 40 km/h. The methodology in Section IV.B.3 is employed and the resulting velocity profiles with different coasting distances D_s are shown in Fig. 9. It shows that deceleration without coasting provides higher recovery of energy (i.e. Blue line in Fig. 9. However, this solution reaches final velocity at a distance of 300m and then cruises for the next 200 meters, which is not desirable.

The dotted line with $D_s = 300$m is the shortest cruising time where no coasting occurs at the end of the trajectory, so it selected as the preferred solution according to the methodology in Section IV.B.3. It is observed that the energy recovery is about 2 kW less than the optimum solution when the cruising in low velocity no longer exists.

So far, the long-term optimised trajectory has been discussed. The trajectory is calculated using an analytical solution and can be updated in real-time. The advantages of the proposed method include fast computational time and consideration of the constraints for the control variables.

C. SHORT-TERM Eco AND SAFE MPC OPTIMISATION

In this section, the proposed EcoSafe-MPC for EVs is tested. A 10-minute highway-urban mix traffic driving scenario, which has a hat-shaped speed limit, was used for this study. The preceding vehicle has a velocity profile similar to Fig. 10a (yellow line), and the following vehicle is driven using EcoSafe-MPC. It is assumed that the information of the preceding vehicle is available through Radar, LIDAR or C-ITS to capture the behaviour of the leading vehicle and $\text{TIV}_{\text{min}} = 2$ and $\text{TTC}_{\text{min}} = 6$ seconds. The EcoSafe-MPC requires a prediction of the preceding vehicle in the optimisation horizon. The preceding vehicle behaviour is predicted using a constant acceleration approximation. The optimum distance for regenerative braking is used to increase the efficiency of regenerative braking during deceleration phases. The blended braking Fig. 10 shows the velocity profile, in distance of travel, along with control variables. It can be seen that the range of acceleration applied is within the defined range when torque is bounded with T_{min} and T_{max}, consistent with the control constraints analytically defined in Section IV. Furthermore, Fig. 10(d) shows that regenerative braking is used to decelerate, except for two instances: at 1700 m when the vehicle reacts to the deceleration of the preceding vehicle and at 10, 110 m at the end of the trip for a full stop. The proposed strategy does not extend the driving time significantly (by 7 seconds) while saving 5.2% of energy compared to the preceding vehicle when the speed limit was chosen as the comfort velocity v_c.

In order to examine the effect of the comfort velocity, the proposed method is tested by varying the comfort velocity as:

$$v_c = (1 - \tau)V_{limit} \tag{29}$$

where $0 \leq \tau \leq 1$ represents the intention of the driver to accept reduced velocity from the speed limit (possibly to save energy). The value of τ can simply be defined by the driver. For example, $\tau = 0.1$ shows that the driver is willing to reduce speed by 10% of the speed limit to save energy.

TABLE 2 shows the effect of choosing the different value of τ. It is observed that by reducing the speed, more energy can be saved. TABLE 2 shows that a 10% speed reduction and an increase in travel time by half a minute can save $\sim$10% energy. Indeed, this $\sim$10% reduction is achievable by increasing 5% of travel time for the selected driving scenario. A further in-depth look at Table 2 shows that the driving behaviour of the preceding vehicle has an impact on the energy saving of the ego vehicle. When the speed

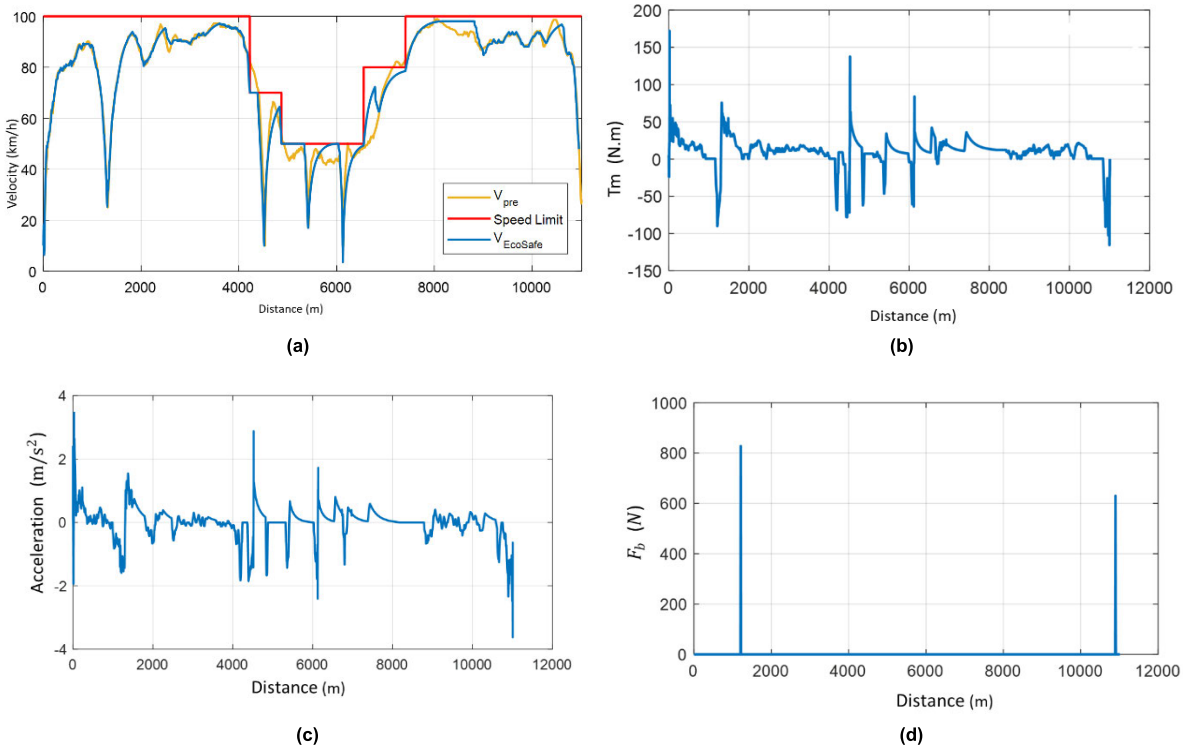

FIGURE 10. Control values for the tested scenario. (a): Velocity profile of preceding vehicle (Blue line), ego-vehicle utilised with EcoSafe-MPC (Green line), and speed limit (Red line). (b): Motor torque on travel distance for ego-vehicle using EcoSafe-MPC. (c): Acceleration of ego-vehicle using EcoSafe-MPC. (d): hydraulic brake applied by EcoSafe-MPC.

TABLE 2. Comparison of Driving Time and Percentage of Energy Saving for Different Intention of the Driver (τ)

τ	Averaged speed	Travel time	Energy consumption	Improvement %	
	Km/h	Minutes	kW.h	EV	ICEV
0%	67.9	9.88	1130	5.2	6.1
5%	67.2	10.03	1122	5.9	8.0
10%	64.8	10.38	1080	9.4	12.3
15%	62.3	10.8	1036	13.4	16.1
20%	59.1	11.3	988	16.6	16.7
25%	55.7	12.1	944	21.8	16.0

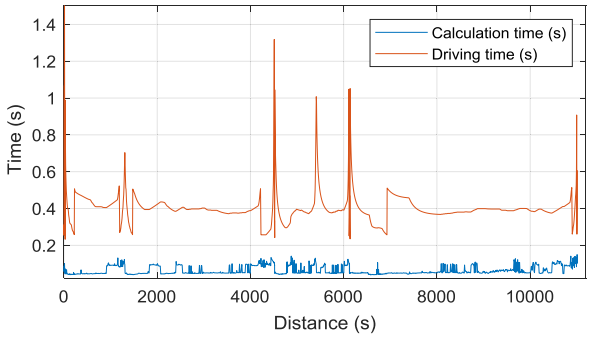

FIGURE 11. Computation demand of the proposed MPC framework.

decreases from the initial velocity to 95% of the speed limit (i.e. $\tau = 0.05$), the energy consumption reduction is very small compared with the other results. This is because the preceding vehicle is often driving less than the speed limit (see Fig. 10a) and the velocity of the ego vehicle is still largely limited by the preceding vehicle.

The same driving scenario for ICEVs is also considered for comparison. The same ICEV dynamics from [16] are used to simulate the driving scenario in Fig. 10a. The same comfort velocity v_c (for a given τ) was used for the ICEV as for the EV. The results are shown in TABLE 2, where it can be seen that EVs and ICEVs have the same performance when the speed limit is chosen as comfort velocity. However, by increasing the τ value, ICEVs showed a better performance until $\tau = 0.2$. For $\tau > 0.2$, the EV outperforms ICEV.

This performance is related to the steady-state optimum velocity of driving for a different vehicle. Indeed, the optimum speed of the ICEV is equal to 58 km/h for the selected vehicle dynamics and driving around this point has better performance. However, for the chosen EV (Table 1), the optimum speed is 18 km/h.

Finally, Fig. 11 shows the computational demand of the proposed algorithm in MATLAB on a PC with Core-i7 CPU and 16 MB of RAM. The CPU time required for one calculation of the optimal controls, including the long-term optimisation and the subsequent MPC-based short

term adaptation. The result shows that the proposed method required 0.0638 seconds of calculation on average with a standard deviation of 0.0238 seconds, and it is always significantly less than the driving time.

VII. CONCLUSION AND FUTURE WORK

In this article, an energy-efficient optimisation was developed for electric vehicles. It is based on a model predictive control, combining long-term optimisation and short-term adaptation. This model takes into account regenerative braking by reframing the analytical solution for long-term optimisation. An analytical solution was developed with low computational demand. Pontryagin's Maximum Principle (PMP) was used to solve for the energy optimal velocity profile for EVs under control constraints. The acceleration was used as the control, and it was bounded in the safe range by augmenting the running cost with the equality constraints. The deceleration problem was then divided into two possible situations: one where only regenerative braking is used or a combination of regenerative braking and hydraulic braking is required. The proposed analytical solution recovers 98% of the optimal energy recovery and has the advantage of providing a fast computation. The proposed MPC approach for EVs was also evaluated. The simulation results for a sample scenario shows that with the proposed EcoSafe-MPC, very little hydraulic braking was used, and the deceleration occurred primarily using regenerative braking, and resulted in a 5% energy savings while the travel time did not increase significantly. The performance of EVs with ICEVs was also compared for the same driving scenario. The results highlighted that eco-driving with EVs is 10% more efficient at lower speeds compared to ICEVs. Indeed, EVs are more efficient at lower speeds, suggesting that better fuel savings can be obtained in urban scenarios rather than highways and motorways with EVs, due to lower speed limits and higher likelihood of using regenerative braking in traffic.

The future work of this research is to consider more sophisticated model for the limits of regenerative braking, e.g. due to battery inefficiencies, temperature effects, etc. Moreover, different aspects of safety, including rear-end collision risk and anticipating the behaviour of the vehicle behind, can also be considered in the MPC framework. The proposed approach can consider the use of cooperative Intelligent Transportation Systems (C-ITS) to obtain more accurately steady-state velocity of upcoming traffic. C-ITS can also be used for better planning of the trajectory.

REFERENCES

[1] L. Pérez-Lombard, J. Ortiz, and C. Pout, "A review on buildings energy consumption information," *Energy Buildings*, vol. 40, no. 3, pp. 394–398, Jan. 2008.

[2] P. Hertzke, N. Müller, S. Schenk, and T. Wu, "The global electric-vehicle market is amped up and on the rise," *McKinsey Center Future Mobility*, pp. 1–8, Nov. 2018.

[3] M. A. A. Abdelkareem, L. Xu, M. K. A. Ali, A. Elagouz, J. Mi, S. Guo, Y. Liu, and L. Zuo, "Vibration energy harvesting in automotive suspension system: A detailed review," *Appl. Energy*, vol. 229, pp. 672–699, Nov. 2018.

[4] A. Vahidi and A. Sciarretta, "Energy saving potentials of connected and automated vehicles," *Transp. Res. C, Emerg. Technol.*, vol. 95, pp. 822–843, Oct. 2018.

[5] G. S. Larue, A. Rakotonirainy, S. Demmel, and H. Malik, "Fuel consumption and gas emissions of an automatic transmission vehicle following simple eco-driving instructions on urban roads," *IET Intell. Transp. Syst.*, vol. 8, no. 7, pp. 590–597, Nov. 2014.

[6] H. Lim, C. C. Mi, and W. Su, "A distance-based two-stage ecological driving system using an estimation of distribution algorithm and model predictive control," *IEEE Trans. Veh. Technol.*, vol. 66, no. 8, pp. 6663–6675, Aug. 2017.

[7] A. Sciarretta, G. D. Nunzio, and L. L. Ojeda, "Optimal ecodriving control: Energy-efficient driving of road vehicles as an optimal control problem," *IEEE Control Syst.*, vol. 35, no. 5, pp. 71–90, Oct. 2015.

[8] L. Guo, H. Chen, Q. Liu, and B. Gao, "A computationally efficient and hierarchical control strategy for velocity optimization of on-road vehicles," *IEEE Trans. Syst., Man, Cybern. Syst.*, vol. 49, no. 1, pp. 31–41, Jan. 2019.

[9] E. Ozatay, U. Ozguner, and D. Filev, "Velocity profile optimization of on road vehicles: Pontryagin's maximum principle based approach," *Control Eng. Pract.*, vol. 61, pp. 244–254, Apr. 2017.

[10] W. Dib, A. Chasse, P. Moulin, A. Sciarretta, and G. Corde, "Optimal energy management for an electric vehicle in eco-driving applications," *Control Eng. Pract.*, vol. 29, pp. 299–307, Aug. 2014.

[11] S. Xie, X. Hu, Z. Xin, and J. Brighton, "Pontryagin's minimum principle based model predictive control of energy management for a plug-in hybrid electric bus," *Appl. Energy*, vol. 236, pp. 893–905, Feb. 2019.

[12] J. Han, A. Sciarretta, L. L. Ojeda, G. De Nunzio, and L. Thibault, "Safe- and eco-driving control for connected and automated electric vehicles using analytical state-constrained optimal solution," *IEEE Trans. Intell. Vehicles*, vol. 3, no. 2, pp. 163–172, Jun. 2018.

[13] Z. Wang and J. Wang, "Ultra-local model predictive control: A model-free approach and its application on automated vehicle trajectory tracking," *Control Eng. Pract.*, vol. 101, Aug. 2020, Art. no. 104482.

[14] D. Lang, T. Stanger, R. Schmied, and L. del Re, "Predictive cooperative adaptive cruise control: Fuel consumption benefits and implementability," in *Optimization and Optimal Control in Automotive Systems*. Cham, Switzerland: Springer, 2014, pp. 163–178.

[15] D. Moser, R. Schmied, H. Waschl, and L. del Re, "Flexible spacing adaptive cruise control using stochastic model predictive control," *IEEE Trans. Control Syst. Technol.*, vol. 26, no. 1, pp. 114–127, Jan. 2018.

[16] S. G. Dehkordi, G. S. Larue, M. E. Cholette, A. Rakotonirainy, and H. A. Rakha, "Ecological and safe driving: A model predictive control approach considering spatial and temporal constraints," *Transp. Res. D, Transp. Environ.*, vol. 67, pp. 208–222, Feb. 2019.

[17] H. Borhan, A. Vahidi, A. M. Phillips, M. L. Kuang, I. V. Kolmanovsky, and S. Di Cairano, "MPC-based energy management of a power-split hybrid electric vehicle," *IEEE Trans. Control Syst. Technol.*, vol. 20, no. 3, pp. 593–603, May 2012.

[18] M. A. S. Kamal, M. Mukai, J. Murata, and T. Kawabe, "On board eco-driving system for varying road-traffic environments using model predictive control," in *Proc. IEEE Int. Conf. Control Appl. (CCA)*, Sep. 2010, pp. 1636–1641.

[19] H. Lim, W. Su, and C. C. Mi, "Distance-based ecological driving scheme using a two-stage hierarchy for long-term optimization and short-term adaptation," *IEEE Trans. Veh. Technol.*, vol. 66, no. 3, pp. 1940–1949, Mar. 2017.

[20] H. Lim and W. Su, "Hierarchical energy management for power-split plug-in HEVs using distance-based optimized speed and SOC profiles," *IEEE Trans. Veh. Technol.*, vol. 67, no. 10, pp. 9312–9323, Oct. 2018.

[21] M. Vajedi and N. L. Azad, "Ecological adaptive cruise controller for plug-in hybrid electric vehicles using nonlinear model predictive control," *IEEE Trans. Intell. Transp. Syst.*, vol. 17, no. 1, pp. 113–122, Jan. 2016.

[22] Y. Huang, E. C. Y. Ng, J. L. Zhou, N. C. Surawski, E. F. C. Chan, and G. Hong, "Eco-driving technology for sustainable road transport: A review," *Renew. Sustain. Energy Rev.*, vol. 93, pp. 596–609, Oct. 2018.

[23] Z. Yi and P. H. Bauer, "Energy aware driving: Optimal electric vehicle speed profiles for sustainability in transportation," *IEEE Trans. Intell. Transp. Syst.*, vol. 20, no. 3, pp. 1137–1148, Mar. 2019.

[24] S. G. Dehkordi, G. S. Larue, M. Cholette, and A. Rakotonirainy, "Benefit assesment of an ecological and safe driving strategy using naturalistic driving data," in *Proc. IEEE Intell. Vehicles Symp. (IV)*, Changshu, China, Jun. 2018, pp. 1931–1936.

[25] S. A. Sajadi-Alamdari, H. Voos, and M. Darouach, "Ecological advanced driver assistance system for optimal energy management in electric vehicles," *IEEE Intell. Transp. Syst. Mag.*, vol. 12, no. 4, pp. 92–109, Nov. 2020.
[26] S. A. Sajadi-Alamdari, H. Voos, and M. Darouach, "Nonlinear model predictive control for ecological driver assistance systems in electric vehicles," *Robot. Auto. Syst.*, vol. 112, pp. 291–303, Feb. 2019.
[27] Y. Jia, R. Jibrin, Y. Itoh, and D. Görges, "Energy-optimal adaptive cruise control for electric vehicles in both time and space domain based on model predictive control," *IFAC-PapersOnLine*, vol. 52, no. 5, pp. 13–20, 2019.
[28] A. Sciarretta and A. Vahidi, *Fundamentals of Vehicle Modeling*. Cham, Switzerland: Springer, 2020, pp. 33–62.
[29] B. Saerens, "Optimal control based eco-driving," Ph.D. dissertation, Dept. Mech. Eng., Katholieke Universiteit Leuven, Leuven, Belgium, 2012.
[30] S. Lekshmi and P. S. L. Priya, "Mathematical modeling of electric vehicles—A survey," *Control Eng. Pract.*, vol. 92, Nov. 2019, Art. no. 104138.
[31] P. Bonsall, R. Liu, and W. Young, "Modelling safety-related driving behaviour-impact of parameter values," *Transp. Res. A, Policy Pract.*, vol. 39, pp. 425–444, Jun. 2005.
[32] B. Saerens and E. Van den Bulck, "Calculation of the minimum-fuel driving control based on Pontryagin's maximum principle," *Transp. Res. D, Transp. Environ.*, vol. 24, pp. 89–97, Oct. 2013.
[33] D. E. Kirk, *Optimal Control Theory: An Introduction*. Chelmsford, MA, USA: Courier Corporation, 2012.
[34] Y. Zhou, M. E. Cholette, A. Bhaskar, and E. Chung, "Optimal vehicle trajectory planning with control constraints and recursive implementation for automated on-ramp merging," *IEEE Trans. Intell. Transp. Syst.*, vol. 20, no. 9, pp. 3409–3420, Sep. 2019.
[35] A. B. Schwarzkopf and R. B. Leipnik, "Control of highway vehicles for minimum fuel consumption over varying terrain," *Transp. Res.*, vol. 11, no. 4, pp. 279–286, Aug. 1977.

SEPEHR G. DEHKORDI received the B.S. degree in electrical engineering from the Azad University of Najafabad, in 2011, the M.S. degree in control and automation engineering from Universiti Putra Malaysia, in 2015, and the Ph.D. degree from the Queensland University of Technology, in 2019.

Since 2019, he has been a Research Associate with the Centre for Accident Research and Road Safety, QLD, Australia, researching on the Connected Automated Vehicle and Intelligence Transportation System (ITS). His research interests include instrumented and autonomous systems, artificial intelligence and automation, optimization techniques in control theory, and road safety approaches in ITS.

MICHAEL E. CHOLETTE received the B.S. degree in mechanical engineering from the University of Michigan, Ann Arbor, MI, USA, in 2007, and the M.S. and Ph.D. degrees from the University of Texas at Austin, Austin, TX, USA, in 2012. Since 2012, he has been with the Queensland University of Technology (QUT), Brisbane, QLD, Australia, first as a Postdoctoral Fellow with the CRC for Infrastructure and Engineering Asset Management (CIEAM) and then as a Lecturer in 2013. He is currently a Senior Lecturer with the School of Mechanical, Medical and Process Engineering. His current research interests include engineering optimization and engineering asset management, particularly condition-based maintenance.

Dr. Cholette is a member of the Engineers Australia and the International Society of Engineering Asset Management (ISEAM).

GRÉGOIRE S. LARUE received the M.Sc. degree in mathematics from the University of Queensland, Australia, and the M.E. degree from the Ecole Centrale de Lyon, France. In 2006, he joined the Centre for Accident Research and Road Safety–Queensland, Queensland University of Technology. He is currently a Senior Research Fellow in road safety and intelligent transport systems. He has worked on a range of industrial and government projects focusing on evaluating how road users react to new technologies.

ANDRY RAKOTONIRAINY is currently the Deputy Director of CARRS-Q and Intelligent Transport System Human factor research program within CARRS-Q. He has 20 years of research and management experience in computer science and brings advanced expertise in road safety and ITS. He has authored more than 220 internationally refereed articles in prestigious conferences and journals. His research has made extensive use of driving simulators, traffic simulators, and instrumented vehicles for developing system prototypes, assessing cost-benefits, understanding human errors, and evaluating system deployment.

SÉBASTIEN GLASER received the Ph.D. degree in automatic and control (defining a driving assistance system in interaction with the driver) in 2004. He was a Researcher in the Development of Connected and Automated Vehicles (CAV). He is currently a Professor of intelligence transportation system with CARRS-Q, QUT. He is also doing research on AV interaction with road users and innovative methods to improve this relationship. He is also managing the Cooperative Highly Automated Driving Safety Study (CHAD) project with the Queensland Department of Transport and Main Roads and iMOVE-CRC.